

# Variable Regions of Antibodies and T-Cell Receptors May Not Be Sufficient in Molecular Simulations Investigating Binding

Bernhard Knapp,<sup>\*,†,‡,§</sup> James Dunbar,<sup>†,§</sup> Marta Alcalá,<sup>‡</sup> and Charlotte M. Deane<sup>†</sup>

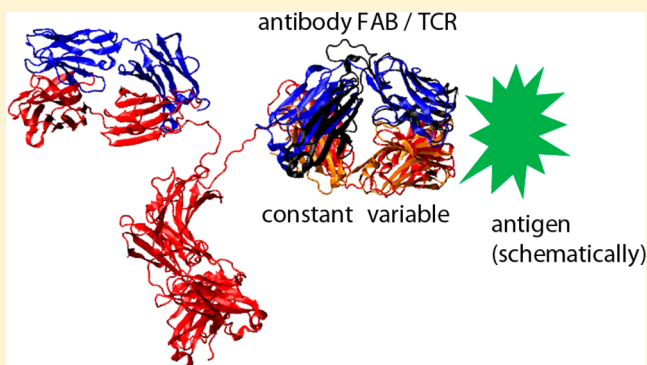
<sup>†</sup>Department of Statistics, Protein Informatics Group, University of Oxford, Oxford OX1 3BD, U.K.

<sup>‡</sup>Department of Basic Sciences, Faculty of Medicine and Health Sciences, International University of Catalonia, 08195 Sant Cugat del Vallès, Barcelona, Spain

<sup>§</sup>Pharma Research and Early Development, Large Molecule Research, Roche Innovation Center Munich 82377 Penzberg, Germany

**S** Supporting Information

**ABSTRACT:** Antibodies and T-cell receptors are important proteins of the immune system that share similar structures. Both contain variable and constant regions. Insight into the dynamics of their binding can be provided by computational simulations. For these simulations the constant regions are often removed to save runtime as binding occurs in the variable regions. Here we present the first study to investigate the effect of removing the constant regions from antibodies and T-cell receptors on such simulations. We performed simulations of an antibody/antigen and T-cell receptor/MHC system with and without constant regions using 10 replicas of 100 ns of each of the four setups. We found that simulations without constant regions show significantly different behavior compared to simulations with constant regions. If the constant regions are not included in the simulations alterations in the binding interface hydrogen bonds and even partial unbinding can occur. These results indicate that constant regions should be included in antibody and T-cell receptor simulations for reliable conclusions to be drawn.



## INTRODUCTION

Human antibodies are large Y-shaped proteins that are used by the immune system to defend against threats such as viruses or bacteria.<sup>1</sup> The two arms of the Y are called fragment antigen-binding (FAB) regions. Each FAB region consists of a heavy and light chain that are both subdivided into a constant and a variable region. In this manuscript the term “constant antibody region” refers only to the constant parts of the FAB region (sometimes also named CH1/CL). For the constant fragment crystallizable regions,<sup>1</sup> we use Fc. The angle between the variable and constant regions is termed the elbow angle.<sup>2,3</sup> The antibody structure is illustrated in Figure 1A. Antibody modes of operation include neutralization in which a part of an antigen surface is blocked, agglutination in which assemblies of antibodies trigger phagocytosis, precipitation in which assemblies of antibodies force antigens to precipitate out of solution, and complement system activation. Antibodies can act in their soluble form without being bound to a cell membrane and can recognize discontinuous antigens.<sup>1</sup>

T-cell receptors (TCRs) are membrane bound surface receptors of T-cells that recognize antigenic peptides in the major histocompatibility complex (MHC) on the surface of antigen-presenting cells. TCRs consist of an  $\alpha$ -chain and a  $\beta$ -chain that are both subdivided into a variable and a constant region. The variable regions of the  $\alpha$ -chain and  $\beta$ -chain are in

contact with the antigen and the MHC (Figure 1B).<sup>4</sup> In contrast to antibodies TCRs only recognize small and continuous peptide antigens that are presented via the MHC of antigen presenting cells to them. TCRs do not act directly against antigens but trigger a signaling cascade inside the T-cell for further actions.<sup>1</sup>

Despite their different modes of action antibodies and TCRs share a similar structure (Figure 1C).<sup>5</sup> Both complexes are known to consist of genetically variable regions with hyper-variable complementary determining region (CDR) loops acting as recognition sensors for antigens.<sup>6</sup> Apart from being genetically hypervariable these regions are often assumed to be structurally flexible particularly between their bound and unbound conformations.<sup>7</sup> Insight into the flexibility of these regions is often desired. Due to the current limitations of experimental techniques computational techniques are frequently used to investigate flexibility of both antibodies and TCRs (reviewed in ref 8). Examples include antibody humanisation,<sup>9</sup> effects of TCR binding on MHC,<sup>10</sup> or immunogenic and nonimmunogenic TCR/peptide/MHC interactions.<sup>11</sup>

These systems are relatively large and therefore present a challenge for molecular simulation. Several approaches to address this challenge have been proposed.<sup>8</sup> They include

**Received:** January 25, 2017

**Published:** June 15, 2017

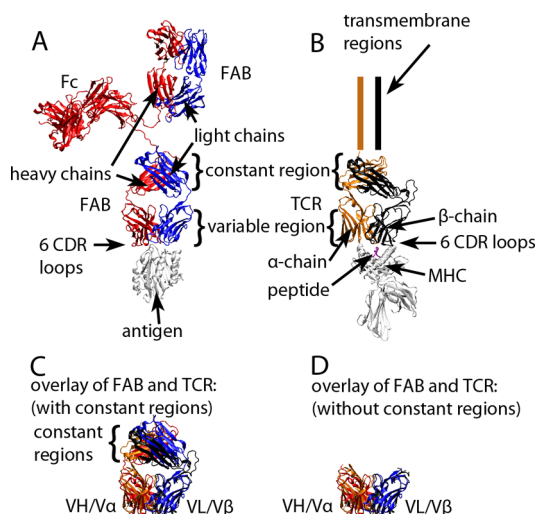


**Figure 1.** Similarity between antibody (PDB ID 1IGT) and T-cell receptor (PDB ID 1OGA). (A) Heavy chain (red) and light chain (blue) of an antibody in complex with an antigen (white). The antigen location was modeled based on PDB ID 1MHP, as a structure of a whole antibody in complex with an antigen is not available. The antibody consists of two fragment antigen-binding (FAB) and one fragment crystallizable (Fc) region. Each FAB region has six CDR loops as main contact sites with the antigen (B)  $\alpha$ -chain (orange) and  $\beta$ -chain (black) of a TCR in complex with MHC (white) and presented peptide (magenta). The putative anchoring of the TCR via transmembrane regions on the surface of a T-cell is shown as two parallel lines. (C) Overlay of antibody and TCR using the variable and constant regions. The heavy chain of the antibody is overlaid with the  $\alpha$ -chain of the TCR while the light chain is overlaid with the  $\beta$ -chain. Only the FAB region of the antibody and the TCR without transmembrane regions is shown. (D) Same as part C but only the variable and not the constant regions are shown. In this study we compare the antigen binding of setup C with the antigen binding of setup D.

bond length constraints,<sup>12</sup> increased masses,<sup>13</sup> virtual sites,<sup>14</sup>  $n$ -bead models,<sup>15</sup> the movement of whole rigid protein regions,<sup>16</sup> temperature modulation,<sup>17</sup> or steered simulations.<sup>18</sup>

An alternative approach to reduce computational costs is to reduce the size of the system that will be simulated. This is often seen practice for both antibodies and TCRs where only the variable regions are simulated<sup>8,9,19–23</sup> as only these domains are in direct contact with the antigen and frequently a structure of the constant regions is not available (605 of the 2668 antibody X-ray structures listed in the SabDab<sup>24</sup> do not contain constant regions). Not including the constant regions saves a considerable amount of computation time. For example, for the AQC2 antibody in complex with an antigen the number of residues shrinks by about 33% and the number of water molecules needed for solvation by about 53%. From here on we refer to the variable part of the heavy antibody chain as VH, the variable part of the light antibody chain as VL, the variable part of the TCR  $\alpha$ -chain as V $\alpha$ , the variable part of the TCR  $\beta$ -chain as V $\beta$ , and the variable and constant regions of one antibody arm as FAB (compare Figure 1C).

In this study we investigated if the removal of constant regions from antibodies and TCRs (compare Figure 1C and D) affects the simulation outcomes at the CDR/antigen interface. We performed simulations of the AQC2 antibody in complex with an antigen<sup>25</sup> as well as the JM22 TCR in complex with peptide/MHC.<sup>26</sup> Both systems were simulated multiple times with and without the constant regions present.

We have investigated only two systems (one antibody and one TCR) but found significant differences between simulations with and without constant regions in both systems. If no constant regions were present we observed a partial detachment between antibody and antigen. A similar behavior occurred for TCR/MHC simulations. It is likely that such differences will exist for many antibody/antigen and TCR/MHC simulations.

## METHODS

**Modeling of the Structures.** We use the I domain of the  $\alpha$ 1 $\beta$ 1 integrin and the FAB fragment of humanized AQC2 antibody with PDB ID 1MHP<sup>25</sup> as an example antibody. It contains both the variable and constant domains as well as a bound antigen. It also displays a very typical orientation between the heavy and light chain as measured by the AB-angle method for antibodies.<sup>27</sup> The system consists of 615 residues where 184 belong to the antigen, 219 to the heavy chain, and 212 to the light chain of the antibody. Computational solvation in a dodecahedral simulation box with a minimum distance of 1.5 nm between protein and box boundary requires 55 165 water molecules. If the constant regions of the antibody are removed the system size reduces to 406 residues (66.0% of the original complex) of which 117 are forming the heavy chain (only VH) and 105 the light chain (only VL) of the antibody. In this case computational solvation in a dodecahedral simulation box with a minimum distance of 1.5 nm between protein and box boundary requires 25 586 water molecules (46.4% of the original complex).

The TCR system is the JM22 TCR bound to HLA-A\*02:01 with PDB ID 1OGA.<sup>26</sup> This system is a well investigated model<sup>26,28</sup> that contains the variable and constant TCR domains as well as a bound MHC. The orientation between the  $\alpha$ - and  $\beta$ -chain is fairly typical for a TCR as measured by the AB-angle method for TCRs.<sup>5</sup> It consists of 824 residues where 376 belong to MHC/B2M, 9 to the peptide antigen, 199 to the  $\alpha$ -chain, and 240 to the  $\beta$ -chain of the TCR. Computational solvation in a dodecahedral simulation box with a minimum distance of 1.5 nm between protein and box boundary requires 99 573 water molecules. If the constant regions of the TCR are removed the system size reduces to 603 residues (73.2% of the original complex) of which 108 are forming the  $\alpha$ -chain (only V $\alpha$ ) and 110 the  $\beta$ -chain (only V $\beta$ ) of the TCR. In this case computational solvation in a dodecahedral simulation box with a minimum distance of 1.5 nm between protein and box boundary requires 56 398 water molecules (56.6% of the original complex).

**Molecular Dynamics Simulations.** Molecular dynamics (MD) simulations were carried out using GROMACS 4<sup>14</sup> and the GROMOS force field in the 53a6 parametrization.<sup>29</sup> All four complexes (antibody with and without constant regions (but never the Fc constant regions) and TCR with and without constant regions) were inserted into dodecahedral simulation boxes with a minimum distance of 1.5 nm between protein and box boundary. The simulation boxes were filled with explicit SPC water. Water molecules were replaced with Na<sup>+</sup> and Cl<sup>−</sup> ions until a salt concentration of 0.15 mol/L and a neutral charge were reached. The solvated systems were energetically minimized using the steepest descent method. Next, the systems were warmed up to 310 K using position restraints. Finally, production runs of 100 ns were carried out using the Oxford Advanced Research Computing (ARC) facility.

It has previously been shown that simulations with identical parametrizations can lead to significantly different trajectories if different seeds are used.<sup>10,17,30,31</sup> Therefore, we performed 10

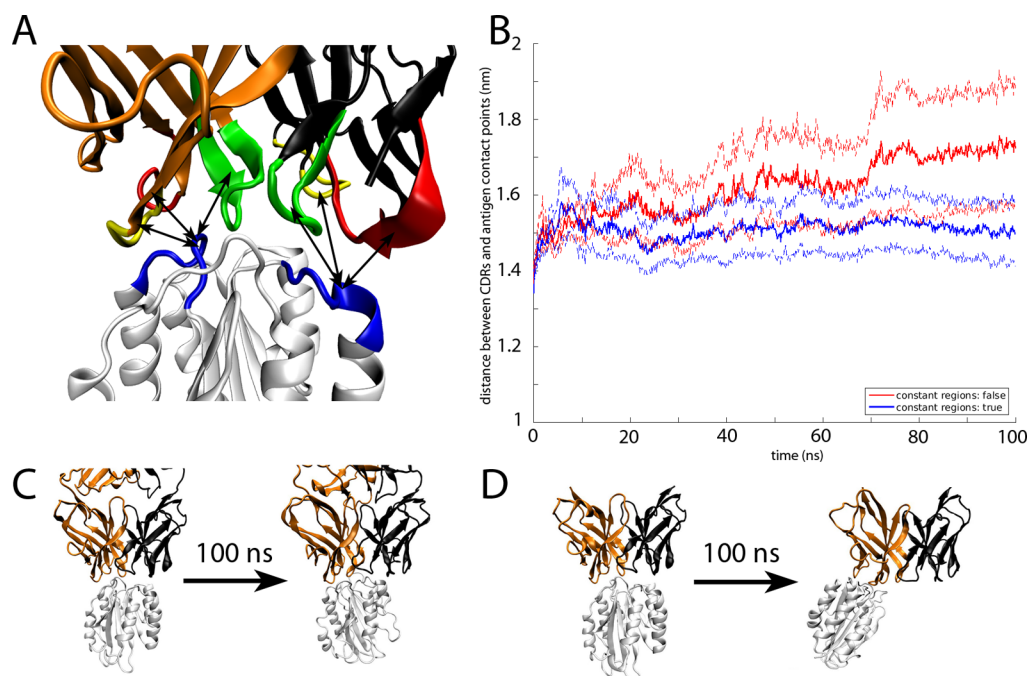


**Figure 2.** Distance between antibody and antigen. (A) Illustration of the distance measure method shown over time of (B). The distances between CDR1 (red), CDR2 (yellow), CDR3 (green) and a close antigen loop (blue; residues 156–162 for the heavy chain and residues 260–265 for the light chain) are measured. By measuring only 6 distances instead of all 12 possible combinations, this analysis is also able to detect a twist of the antigen. (B) Average values of all the distances shown in part A over time grouped by the presence of constant regions. The dashed thin lines indicate the standard error of mean over the 10 replicas. The distance increase can be related to the antigen detachment of several replicas without constant regions. (C) Example of a stable simulation with constant regions present with the starting configuration on the left and the last frame of a 100 ns simulation on the right. Only a small part of the constant regions is illustrated, but simulations were performed with the whole constant regions. (D) Same as part C but without constant regions. Similar schemes as parts C and D but for all replicas are shown in Figure S1: (orange) antibody heavy chain; (black) antibody light chain; (white) antigen.

replicas of each simulation. The total simulation time was 4  $\mu$ s (100 ns  $\times$  4 systems  $\times$  10 replicas).

**Methods of Trajectory Evaluation.** The GROMACS<sup>14</sup> tools *g\_dist*, *h\_bond* and *g\_rms* were used to calculate distance, hydrogen bond (H-bond) and root-mean-square deviation (RMSD) metrics. The *gro2mat* package<sup>32</sup> was used to import data into Matlab 8.5 where plotting and analysis<sup>33</sup> was done. Simulations were manually inspected with VMD<sup>34</sup> and the *vmdICE* plugin.<sup>35</sup>

**Magnitude of Difference between Simulations.** In this study the total variation distance (tvd) is used to quantify how different simulations with and without constant regions are. In our previous study<sup>11</sup> we defined the tvd as

$$\text{tvd}(f_1, f_2) = \frac{1}{2} \int |f_1(x) - f_2(x)| dx$$

Where  $f_1(x)$  is the first distribution normalized and  $f_2(x)$  the second distribution normalized. Thus, the tvd values can range between 0 and 1. A value of 0 represents perfect overlap (0% variation) of the distributions while a value of 1 represents no overlap (100% variation).

The tvd describes distribution overlaps but not a quantification of the difference in mean values. Hence, we also calculated a normalized distance between the means of the distributions according to ref 11. This value is referred to as  $d/r$  and defined as

$$d/r = \frac{|\bar{X}_1 - \bar{X}_2|}{\text{range}(X_{1;2.5-97.5\%} \cup X_{2;2.5-97.5\%})}$$

Where  $\bar{X}_1$  and  $\bar{X}_2$  are the mean value of the two distributions (with and without constant regions) and the denominator is the

range of the combined distributions excluding the lowest and highest 2.5%.

## RESULTS

In total we analyzed 20 antibody/antigen and 20 TCRpMHC simulations each of 100 ns in length. Ten of each were carried out with constant regions and 10 without. The Fc regions of the antibody were not included in any of the simulations.

**Time for Computation.** Using six nodes with 16 cores each a 100 ns simulation took 33.38 ( $\pm 1.59$ ) h for antibody/antigen simulations with constant regions. Without constant regions this value dropped to 23.85 ( $\pm 7.05$ ) h. This is 71.42% of the runtime (66% of the number of amino acids and 46.4% of the water molecules). The increase in speed of the TCR/MHC simulations without constant regions was similar.

**Constant Regions Stabilize Binding between Antibody and Antigen.** To quantify the binding stability between antibody and antigen we measured the distances between the CDRs of each antibody chain and two loops of the antigen that are in close proximity to the CDR loops (Figure 2A). Using this metric we found that in simulations without constant regions the antibody and the antigen tend to detach from each other more rapidly and more often than in simulations with constant regions (Figure 2B). An example is shown in Figure 2C and D. The images for all 20 simulations are shown in Figure S1.

Another way to quantify such detachment processes are H-bonds. Analyzing our simulations for H-bond presence between the antigen, heavy chain, and light chain of the antibody yields a similar conclusion as the distance metric: if no constant regions are present, the number of H-bonds between antibody and



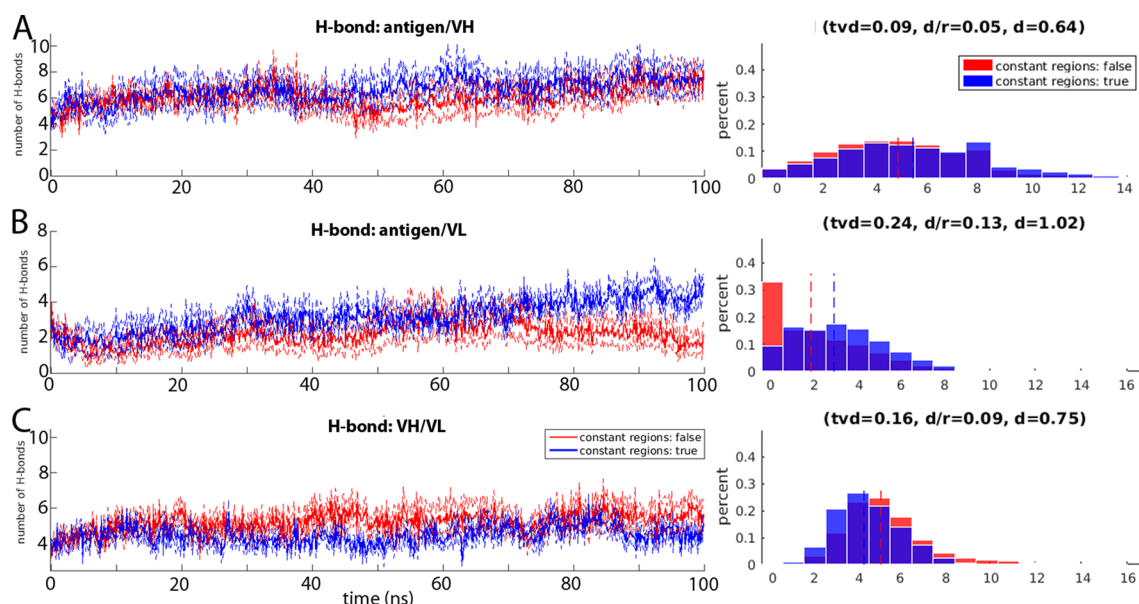


**Figure 3.** H-bonds antibody and antigen. (A) H-bonds between the antigen and VH of the antibody. (B) H-bonds between the antigen and VL of the antibody. (C) H-bonds between VH and VL of the antibody. The dashed thin lines indicate the standard error of mean over the 10 replicas. The histograms on the right side show the same data as the line plots on the left side. The dashed lines in the histograms indicate mean values.

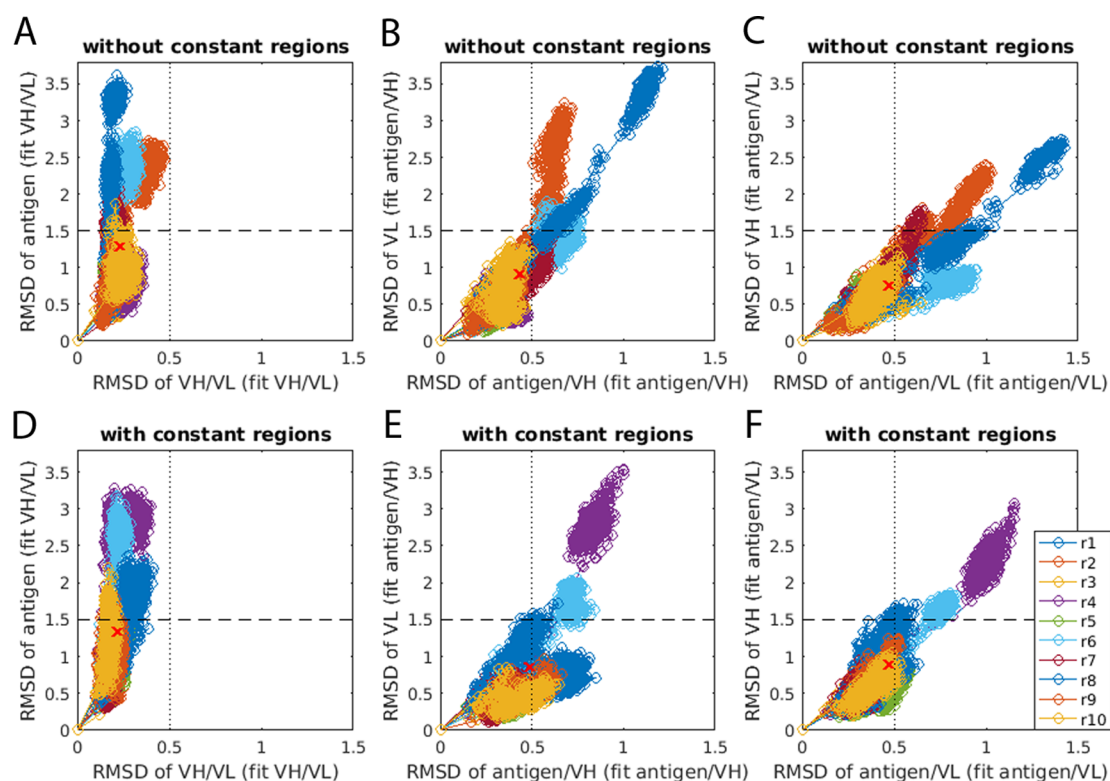


**Figure 4.** RMSD (nm) analysis to determine which subunit of the antibody/antigen detaches from which subunit. (A) Fit on VH/VL and plot of antigen against VH/VL based on simulations without constant regions. (B) Fit on antigen/VH and plot of VL against antigen/VH based on simulations without constant regions. (C) Fit on antigen/VL and plot of VH against antigen/VL based on simulations without constant regions. (D) Fit on VH/VL and plot of antigen against VH/VL based on simulations with constant regions. (E) Fit on antigen/VH and plot of VL against antigen/VH based on simulations with constant regions. (F) Fit on antigen/VL and plot of VH against antigen/VL based on simulations with constant regions. Different replicas are shown in different colors. When fitting on VH/VL the VH/VL RMSD never exceeds 0.5 nm; this is indicated by a vertical dotted line in all plots. The RMSD of a region on which the fit was performed is expected to be lower in general. This is reflected by the different scaling of the x- and y-axes of all plots. To give an indication of this, the limit of the x-axis (1.5 nm) is illustrated on the y-axis by a horizontal dashed line. The red  $\times$  symbol indicates the mean value over all frames and replicas.

antigen is significantly lower. In the case of VH (Figure 3A), the difference is small while for VL (Figure 3B) the difference is

larger. This becomes even clearer in the histogram at the right side of Figure 3B where we see that about 33% of all frames of

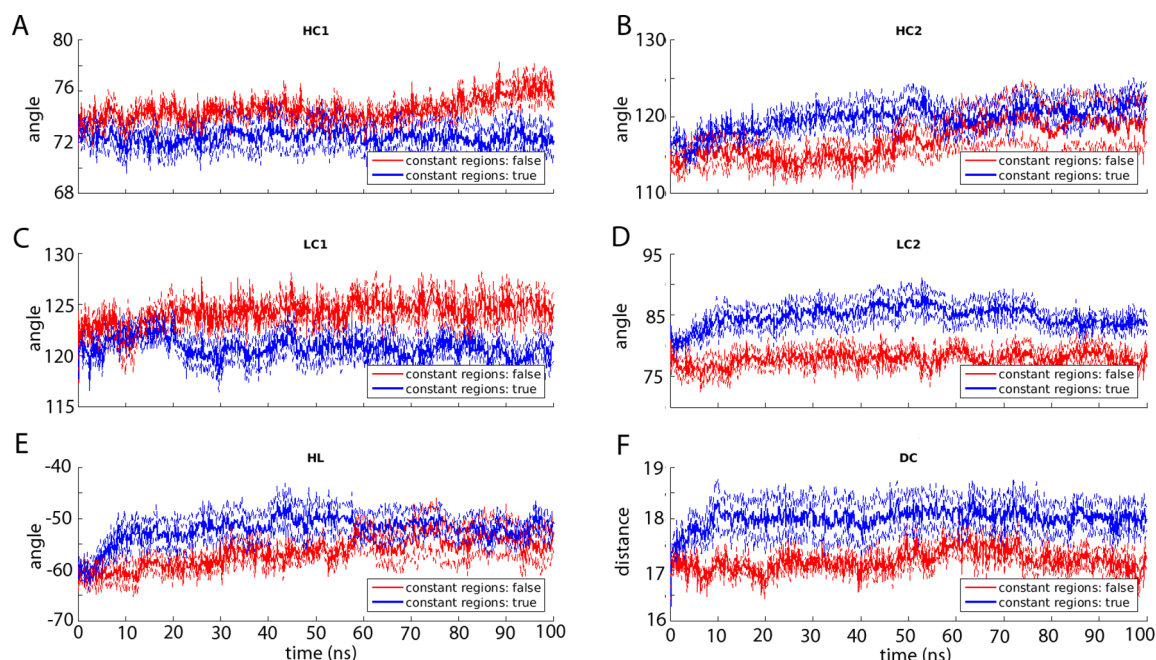


**Figure 5.** Antibody angles between the variable segments of the heavy and light chain. (A) The bend angle, HC1, between H1 and C. (B) The bend angle, HC2, between H2 and C. (C) The bend angle, LC1, between L1 and C. (D) The bend angle, LC2, between L2 and C. (E) The torsion angle, HL, from H1 to L1 measured about C. (F) The length of C, DC. The dashed thin lines indicate the standard error of mean over the 10 replicas. The method is described in detail in the work of Dunbar et al.<sup>27</sup> and illustrated in Figure S4.

simulations without constant regions have zero H-bonds between VL and the antigen while this is only the case for about 10% of the simulation frames with constant regions. This agrees with the generally held view that CDRH3 is the most important interaction site.<sup>36</sup>

These results suggest that without the constant regions the binding between antibody and antigen is less stable. The structural background for the stabilization effect of constant antibody regions is shown in Figure S2.

**Antigen Detaches from the Antibody.** Individual configurations originating from molecular simulations are usually superimposed on a reference structure for visual inspection and analysis. The superimposition (“fitting”) helps to deal with the system rotating around its own axis and/or drifting out of the simulation box on one side and coming back in via periodic boundary conditions on the other side. This fitting step is crucial as it can significantly influence further results.

In our case visualization based on different fitting might give different impressions. To objectively determine which movement occurs we tested all pair wise fitting combinations: Fit on VH/VL and plot the RMSD of the antigen over the RMSD of VH/VL (Figure 4A), fit on antigen/VH and plot the RMSD of VL over the RMSD of antigen/VH (Figure 4B), and fit on antigen/VL and plot the RMSD of VH over the RMSD of antigen/VL (Figure 4C).

In Figure 4A it can be seen that VH and VL are relatively stable in themselves while the antigen drifts from its original position. Figure 4B might create the impression that VL also drifts apart but in this case the antigen and VH are not stable by themselves leading to a shift in the center of mass that impacts the structural alignment preceding the RMSD calculation. For VH, the antigen and VL are not stable by themselves as well (Figure 4C). Simulations with and without constant regions show similar behavior (compare upper and lower rows of Figure 4). This leads to the conclusion that if the antigen/VL/VH complex becomes

unstable the antigen detaches from the antibody while VL and VH stably bind to each other.

This shows that the antigen detaches from the antibody and not the antibody chains from each other.

**Constant Antibody Regions Hold Variable Regions at Distance.** The results above describe how the antigen tends to detach from the antibody if the constant regions are not present. As the constant regions are not in contact with the antigen it must be through the influence of the constant regions on the variable regions. We find that the relative position of VH and VL is influenced by the presence of constant regions. VH and VL tend to be closer without constant regions ( $23.92 \pm 0.13$  Å) than with constant regions ( $24.43 \pm 0.19$  Å) (Figure S3) which is also reflected in the number of H-bonds between VH and VL (Figure 3C). It seems that the constant regions are holding the variable regions in position and therefore stabilize the shape of the interface to the antigen.

This behavior can be seen in detail in the orientation between VH and VL as measured by the AB angle method.<sup>5,27</sup> AB angles describe the orientation between the variable segments of antibodies and TCRs based on five angles and one distance. The AB angle method is graphically illustrated in Figure S4. Simulations with and without constant regions differ from each other in bending and torsion angles between VH and VL (Figure 5). The VH and VL bend angles HC1 and LC1 tend to be larger for simulations without constant regions (Figure 5AC) while the bend angles HC2 and LC2 tend to be larger for simulations with constant regions (Figure 5BD). The torsion angle between VH and VL is slightly lower for simulations without constant regions (Figure 5E). Hereby the AB angles demonstrate how the two sets of simulations occupy different VH–VL orientation spaces but do not necessarily show their spatial closeness to the X-ray structure as different AB angles can counteract against each other. Although some of the angle measures are closer to the X-ray structure for simulations without constant domains the VH/

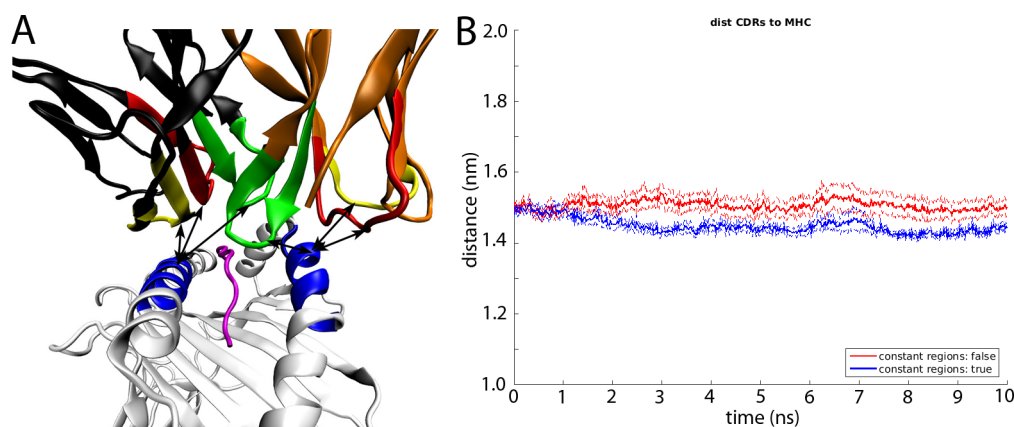


**Figure 6.** Distance between TCR and MHC. (A) Illustrations of the distance measure method shown over time in part B. The distances between CDR1 (red), CDR2 (yellow), CDR3 (green) and two 10 residue long MHC helix segments (blue; residues 152–161 for the  $\alpha$ -chain and residues 65–74 for the  $\beta$ -chain) in close proximity to the CDR loops are measured. By measuring only 6 distances instead of all 12 possible combinations this analysis is also able to detect a twist of the MHC relative to the TCR. (B) Average value of all the distances shown in part A over time group the presence of the constant regions. The dashed thin lines indicate the standard error of mean over the 10 replicas.

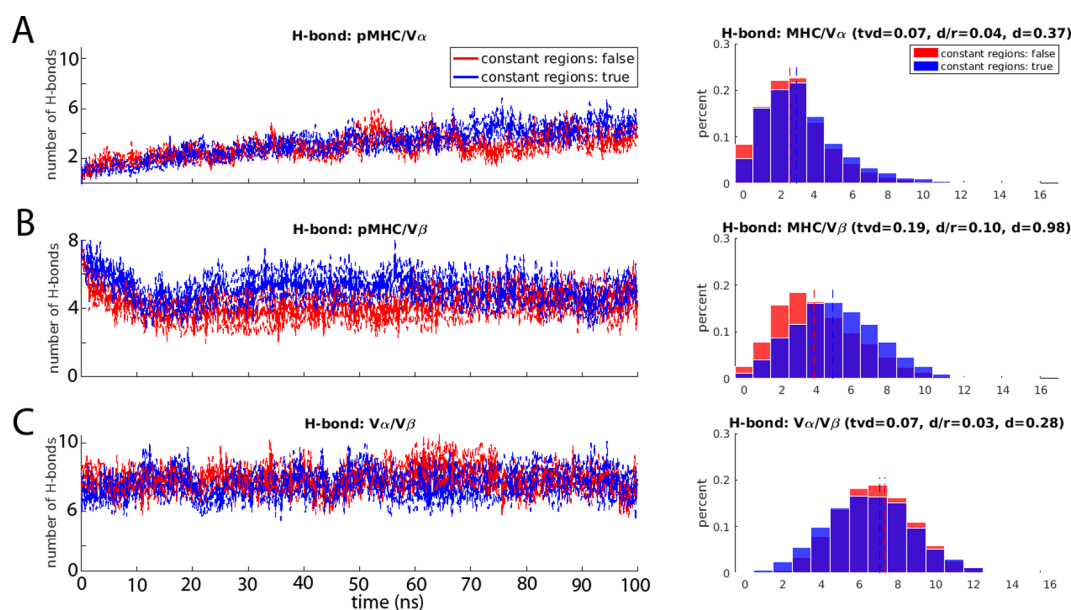


**Figure 7.** H-bonds TCR and pMHC. (A) H-bonds between pMHC and the  $V\alpha$  of the TCR. (B) H-bonds between pMHC and the  $V\beta$  of the TCR. (C) H-bonds between  $V\alpha$  and  $V\beta$ . The dashed thin lines indicate the standard error of mean over the 10 replicas. The histograms on the right side show the same data as the line plots on the left side. The dashed lines in the histograms indicate mean values. All simulations start from the same configuration.

VL structure stays on average more conserved for simulations with constant domain (mean RMSD 0.215 and 0.227 nm and Figure S5).

The distance between conserved residues of VH and VL (Figure 5F) shows a similar but even more pronounced pattern than the distance between the centers of masses of VH and VL (Figure S3): VH and VL in simulations without constant regions are closer.

**Constant Regions Also Stabilize Binding between TCR and MHC.** For TCR/MHC simulations we measured the distances between two segments of the MHC helix and their adjacent CDR loops (Figure 6A). The distance in the binding interface is relatively conserved over time and simulations with constant regions have a slightly decreased interface distance as compared to simulations without constant regions, which indicates tighter binding (Figure 6B). This is caused by a slight movement of the MHC relative to the TCR chains (Figure S8), but no

severe change of binding mode between TCR and MHC was observed. The last frames of all 10 simulations are illustrated in Figure S6.

While the lack of constant regions does not cause a full detachment of the MHC from the TCR, an alteration of the H-bonds in the binding interface is induced (Figure 7). Simulations without constant domains establish fewer additional H-bonds between  $V\alpha$  and MHC (Figure 7A) and loose more H-bonds between  $V\beta$  and MHC than simulations with constant regions (Figure 7B). This lead to the result that  $V\alpha$  has a lower number of H-bonds to the MHC if no constant regions are present (Figure 7A), and this is even more pronounced for the  $V\beta$ /MHC where simulations with constant regions have on average almost one H-bond more than simulations without constant regions (Figure 7B). The number of H-bonds between  $V\alpha$  and  $V\beta$  is marginally increased for simulations without constant regions (Figure 7C).



This indicates that also in the case of the TCR the binding to the MHC is disturbed if no constant TCR regions are present. The structural background for the constant TCR regions' stabilization effect is shown in Figure S7. As the MHC is a large ligand it may well be the case that the unbinding process starts by losing H-bonds but cannot fully progress within the 100 ns of simulation time.

As the slightly increased H-bonds between  $V\alpha$  and  $V\beta$  indicate (Figure 7C) the lack of constant regions makes  $V\alpha$  and  $V\beta$  come closer together. The centers of masses of  $V\alpha$  and  $V\beta$  are on average 23.80 ( $\pm 0.56$ ) Å apart without constant regions and 24.11 ( $\pm 0.49$ ) Å apart with constant regions (Figure S9).

Also the angles between the variable regions are affected by the lack of constant regions (Figure S10). However, similar to the interface distance the changes are subtler than in antibodies. Larger changes are only observable in an increase in the BC1 tilt (Figure S10C) and AB torsion (Figure S10E) as well as a decrease in the distance between conserved  $C\alpha$  atoms of  $V\alpha$  and  $V\beta$  (Figure S10F) consistent with the decreased distance in the center of masses (Figure S9).

This shows that the lack of constant regions causes in principle similar artifacts into TCR/MHC simulations as it does for antibody/antigen simulations. However, due to the much larger binding interface between TCR/MHC the effects take considerably longer to develop fully.

## ■ DISCUSSION

In this study we show that the results of antibody and TCR simulation that do not include constant regions may lead to incorrect results. Here we have only compared one antibody and one TCR system with and without constant regions but as we observe differences it is likely that such differences will exist in many examples. In our systems considerable differences in the binding behavior and H-bonds were found. These differences are caused by an altered arrangement of the antibody and TCR chains. The VH/VL and  $V\alpha/V\beta$  regions are closer to each other and increase their number of H-bonds between each other if no constant regions are present. This leads to a change in the orientation between the two receptor chains and appears to lead to the initialization of an unbinding process of antibody/antigen. In the TCR/MHC simulations no unbinding was observed though interface distances increased slightly, but this slight increase caused differences in the H-bond number between TCR and pMHC. Hence, we conclude that simulations of antibodies or TCRs without constant regions run the risk of artifacts.

This conclusion is also supported by experimental data. It has been shown that constant and variable domains of antibody FAB fragments show significant mutual stabilization<sup>37</sup> and interdomain interactions within antibodies in general contribute to their overall stability.<sup>38,39</sup> The presence of constant domains has been shown to make the variable regions of antibodies more stable and soluble.<sup>40</sup> Therefore, site-directed mutagenesis of constant antibody domains has been used to improve thermodynamics stabilities of the FAB fragment.<sup>41</sup>

In TCRs an early study showed that constant regions are of high importance for  $\alpha$  and  $\beta$  chain assembly.<sup>42</sup> It is also known that not only are the constant regions major structural components of the TCR<sup>4,43</sup> but also pMHC ligation can trigger conformational changes in the A–B loop of the constant TCR  $\alpha$ -chain<sup>44</sup> or rearrangement between the BC and DE  $\beta$ -turns of the constant TCR  $\alpha$ -chain might be a signaling intermediate.<sup>45</sup>

It is hard to predict how the inclusion of the constant region would have affected previous computational studies. However,

on the basis of our results we think that it is likely that constant regions would have increased antibody rigidification in reaction to antigens<sup>19</sup> (see Figures S2 and S7), altered dissociations between heavy and light chain<sup>20</sup> (see Figures S3 and S9), improved CDR refinement (see Figures 2, 3, 6, and 7) and RMSF<sup>23</sup> (see Figures S2 and S7), or improved energy calculations and H-bonds between antibody and antigen<sup>22</sup> (see Figures 2 and 3). Given the importance of variable and constant regions, the question naturally arises whether the variable and constant regions together are sufficient for reliable results and further domains need to be included in simulations (compare Figure 1). Antibodies consist of two FAB regions and one Fc region in total being about 3–4 times larger than the domains simulated in this study. While it would be interesting to see if also the presence of these weakly linked regions influences results further, this experiment is currently not feasible as only few whole antibody structures exist (e.g., PDB IDs 1IGT and 5DK3),<sup>46</sup> and these structures do not contain an antigen. As the linkers between the FAB regions and the Fc regions are long loops, the coupling between them might not be very strong and the FAB regions are thought to have a high flexibility in their orientation relative to the Fc regions. Therefore, modeling of antibodies on the basis of a single structure might introduce more uncertainty into the model than it removes. Once sufficient experimental structural data of whole antibodies is available it should be investigated whether these regions further influence results of structural simulations.

In the case of TCRs the inclusion of transmembrane regions, membranes and coreceptors might be beneficial. However, to date no direct experimental evidence exists on their arrangement. Only one MD study has so far attempted to model these arrangements.<sup>47</sup> The authors modeled the orientation between membrane and receptors as orthogonal which is a reasonable assumption but does not agree with later published SAXS<sup>48</sup> data. These data on the other hand have the limitation that four models fit the data approximately equally well and it is not possible to determine the rotation of the TCR relative to CD3. Hence, the inclusion of membranes and coreceptors currently might also introduce more uncertainties than it resolves.

We conclude that simulations without constant regions can show significantly different behavior compared to simulations with constant regions. If the constant regions are not included in the simulations then alterations in the binding interface and even a partial unbinding can occur. These results indicate that constant regions should be included in antibody and TCR simulations for reliable results.

## ■ ASSOCIATED CONTENT

### 📄 Supporting Information

The Supporting Information is available free of charge on the ACS Publications website at DOI: 10.1021/acs.jctc.7b00080.

Additional analyses of the antibody simulations and the TCR equivalent for every antibody figure (if not given in the main text) (PDF)

## ■ AUTHOR INFORMATION

### Corresponding Author

\*E-mail: science.bernhard.knapp@gmail.com.

### ORCID

Bernhard Knapp: 0000-0002-5714-7105

## Author Contributions

B.K. and C.M.D. conceived and designed the experiments. B.K. performed the experiments. B.K. and M.A. analyzed the data. J.D. implemented an MD version for AB angles. C.M.D. provided computational resources. B.K. wrote the paper. C.M.D. and J.D. revised the paper.

## Funding

This manuscript was funded by the following: 2020 Science Programme (UK Engineering and Physical Sciences Research Council (EPSRC) Cross-Discipline Interface Programme, EP/I017909/1), and EPSRC and Medical Research Council Systems (MRC) Approaches to Biomedical Science Centre for Doctoral Training (EP/L016044/1). J.D. was partly funded by Roche.

## Notes

The authors declare no competing financial interest.

## ACKNOWLEDGMENTS

The authors would like to acknowledge the use of the Oxford Advanced Research Computing (ARC) facility carrying out this work.

## REFERENCES

- (1) Janeway, C. A.; Travers, P.; Walport, M.; Shlomchik, M. J. *Immunobiology*, 6 ed.; Garland Science: 2005.
- (2) Stanfield, R. L.; Zemla, A.; Wilson, I. A.; Rupp, B. Antibody elbow angles are influenced by their light chain class. *J. Mol. Biol.* **2006**, *357* (5), 1566–1574.
- (3) Sela-Culang, I.; Alon, S.; Ofra, Y. A systematic comparison of free and bound antibodies reveals binding-related conformational changes. *J. Immunol.* **2012**, *189* (10), 4890–4899.
- (4) Rudolph, M. G.; Stanfield, R. L.; Wilson, I. A. How TCRs bind MHCs, peptides, and coreceptors. *Annu. Rev. Immunol.* **2006**, *24*, 419–466.
- (5) Dunbar, J.; Knapp, B.; Fuchs, A.; Shi, J.; Deane, C. M. Examining Variable Domain Orientations in Antigen Receptors Gives Insight into TCR-Like Antibody Design. *PLoS Comput. Biol.* **2014**, *10* (9), e1003852.
- (6) Esmailbeiki, R.; Krawczyk, K.; Knapp, B.; Nebel, J.; Deane, C. M. Progress and Challenges in Predicting Protein-Protein Interfaces. *Briefings Bioinf.* **2016**, *17* (1), 117–31.
- (7) Keskin, O. Binding induced conformational changes of proteins correlate with their intrinsic fluctuations: a case study of antibodies. *BMC Struct. Biol.* **2007**, *7*, 31.
- (8) Knapp, B.; Demharter, S.; Esmailbeiki, R.; Deane, C. M. Current Status and Future Challenges in T-cell receptor/peptide/MHC Molecular Dynamics Simulations. *Briefings Bioinf.* **2015**, *16* (6), 1035–1044.
- (9) Margreitter, C.; Mayrhofer, P.; Kunert, R.; Oostenbrink, C. Antibody humanization by molecular dynamics simulations-in-silico guided selection of critical backmutations. *J. Mol. Recognit.* **2016**, *29* (6), 266–275.
- (10) Knapp, B.; Deane, C. M. T-Cell Receptor Binding Affects the Dynamics of the Peptide/MHC-I Complex. *J. Chem. Inf. Model.* **2016**, *56* (1), 46–53.
- (11) Knapp, B.; Dunbar, J.; Deane, C. M. Large Scale Characterization of the LC13 TCR and HLA-B8 Structural Landscape in Reaction to 172 Altered Peptide Ligands: A Molecular Dynamics Simulation Study. *PLoS Comput. Biol.* **2014**, *10* (8), e1003748.
- (12) Mazur, A. K. Hierarchy of Fast Motions in Protein Dynamics. *J. Phys. Chem. B* **1998**, *102*, 473–479.
- (13) Feenstra, K. A.; Hess, B.; Berendsen, H. J. Improving efficiency of large time-scale molecular dynamics simulations of hydrogen-rich systems. *J. Comput. Chem.* **1999**, *20*, 786–798.
- (14) Hess, B.; Kutzner, C.; vanderSpoel, D.; Lindahl, E. GROMACS 4: Algorithms for Highly Efficient, Load-Balanced, and Scalable Molecular Simulation. *J. Chem. Theory Comput.* **2008**, *4* (3), 435–447.
- (15) Minary, P.; Levitt, M. Probing protein fold space with a simplified model. *J. Mol. Biol.* **2008**, *375* (4), 920–933.
- (16) Sim, A. Y.; Levitt, M.; Minary, P. Modeling and design by hierarchical natural moves. *Proc. Natl. Acad. Sci. U. S. A.* **2012**, *109* (8), 2890–2895.
- (17) Knapp, B.; Demharter, S.; Deane, C. M.; Minary, P. Exploring peptide/MHC detachment processes using Hierarchical Natural Move Monte Carlo. *Bioinformatics* **2015**, *32* (2), 181–186.
- (18) Cuendet, M. A.; Zoete, V.; Michielin, O. How T cell receptors interact with peptide-MHCs: a multiple steered molecular dynamics study. *Proteins: Struct., Funct., Genet.* **2011**, *79* (11), 3007–3024.
- (19) Gill, J.; Jayaswal, P.; Salunke, D. M. Antigen exposure leads to rigidification of germline antibody combining site. *J. Bioinf. Comput. Biol.* **2014**, *12* (3), 1450006.
- (20) Wang, T.; Duan, Y. Probing the stability-limiting regions of an antibody single-chain variable fragment: a molecular dynamics simulation study. *Protein Eng., Des. Sel.* **2011**, *24* (9), 649–657.
- (21) Osajima, T.; Suzuki, M.; Neya, S.; Hoshino, T. Computational and statistical study on the molecular interaction between antigen and antibody. *J. Mol. Graphics Modell.* **2014**, *53*, 128–139.
- (22) Osajima, T.; Hoshino, T. Roles of the respective loops at complementarity determining region on the antigen-antibody recognition. *Comput. Biol. Chem.* **2016**, *64*, 368–383.
- (23) Koivuniemi, A.; Takkinen, K.; Nevanen, T. A computational approach for studying antibody-antigen interactions without prior structural information: the anti-testosterone binding antibody as a case study. *Proteins: Struct., Funct., Genet.* **2017**, *85* (2), 322–331.
- (24) Dunbar, J.; Krawczyk, K.; Leem, J.; Baker, T.; Fuchs, A.; Georges, G.; Shi, J.; Deane, C. M. SABDab: the structural antibody database. *Nucleic Acids Res.* **2014**, *42* (D1), D1140–D1146.
- (25) Karpusas, M.; Ferrant, J.; Weinreb, P. H.; Carmillo, A.; Taylor, F. R.; Garber, E. A. Crystal structure of the alpha1beta1 integrin I domain in complex with an antibody Fab fragment. *J. Mol. Biol.* **2003**, *327* (5), 1031–1041.
- (26) Stewart-Jones, G. B.; McMichael, A. J.; Bell, J. I.; Stuart, D. I.; Jones, E. Y. A structural basis for immunodominant human T cell receptor recognition. *Nat. Immunol.* **2003**, *4* (7), 657–663.
- (27) Dunbar, J.; Fuchs, A.; Shi, J.; Deane, C. M. ABangle: characterising the VH-VL orientation in antibodies. *Protein Eng., Des. Sel.* **2013**, *26* (10), 611–620.
- (28) Zhang, H.; Lim, H. S.; Knapp, B.; Deane, C. M.; Aleksic, M.; Dushek, O.; van der Merwe, P. A. The contribution of major histocompatibility complex contacts to the affinity and kinetics of T cell receptor binding. *Sci. Rep.* **2016**, *6*, 35326.
- (29) Oostenbrink, C.; Villa, A.; Mark, A. E.; Van Gunsteren, W. F. A biomolecular force field based on the free enthalpy of hydration and solvation: The GROMOS force-field parameter sets 53A5 and 53A6. *J. Comput. Chem.* **2004**, *25* (13), 1656–1676.
- (30) Wright, D. W.; Hall, B. A.; Kenway, O. A.; Jha, S.; Coveney, P. V. Computing Clinically Relevant Binding Free Energies of HIV-1 Protease Inhibitors. *J. Chem. Theory Comput.* **2014**, *10* (3), 1228–1241.
- (31) Wan, S.; Knapp, B.; Wright, D.; Deane, C.; Coveney, P. V. Rapid, Precise and Reproducible Prediction of Peptide-MHC Binding Affinities from Molecular Dynamics that Correlate Well with Experiment. *J. Chem. Theory Comput.* **2015**, *11* (7), 3346–3356.
- (32) Dien, H.; Deane, C. M.; Knapp, B. Gro2mat: A package to efficiently read Gromacs output in Matlab. *J. Comput. Chem.* **2014**, *35* (20), 1528–1531.
- (33) Hischenhuber, B.; Havlicek, H.; Todoric, J.; Holtrigl-Binder, S.; Schreiner, W.; Knapp, B. Differential geometric analysis of alterations in MH alpha-helices. *J. Comput. Chem.* **2013**, *34* (21), 1862–1879.
- (34) Humphrey, W.; Dalke, A.; Schulten, K. VMD: visual molecular dynamics. *J. Mol. Graphics* **1996**, *14* (1), 33–38.
- (35) Knapp, B.; Lederer, N.; Omasits, U.; Schreiner, W. vmdICE: a plug-in for rapid evaluation of molecular dynamics simulations using VMD. *J. Comput. Chem.* **2010**, *31* (16), 2868–2873.
- (36) Karpusas, M.; Ferrant, J.; Weinreb, P. H.; Carmillo, A.; Taylor, F. R.; Garber, E. A. Crystal structure of the alpha1beta1 integrin I domain



in complex with an antibody Fab fragment. *J. Mol. Biol.* **2003**, 327 (5), 1031–1041.

(37) Rothlisberger, D.; Honegger, A.; Pluckthun, A. Domain interactions in the Fab fragment: a comparative evaluation of the single-chain Fv and Fab format engineered with variable domains of different stability. *J. Mol. Biol.* **2005**, 347 (4), 773–789.

(38) Demarest, S. J.; Glaser, S. M. Antibody therapeutics, antibody engineering, and the merits of protein stability. *Curr. Opin. Drug Discovery Devel.* **2008**, 11 (5), 675–687.

(39) Mabry, R.; Snavely, M. Therapeutic bispecific antibodies: The selection of stable single-chain fragments to overcome engineering obstacles. *IDrugs* **2010**, 13 (8), 543–549.

(40) Wu, X.; Sereno, A. J.; Huang, F.; Lewis, S. M.; Lieu, R. L.; Weldon, C.; Torres, C.; Fine, C.; Batt, M. A.; Fitchett, J. R.; Glasebrook, A. L.; Kuhlman, B.; Demarest, S. J. Fab-based bispecific antibody formats with robust biophysical properties and biological activity. *MAbs* **2015**, 7 (3), 470–482.

(41) Teerinen, T.; Valjakka, J.; Rouvinen, J.; Takkinen, K. Structure-based stability engineering of the mouse IgG1 Fab fragment by modifying constant domains. *J. Mol. Biol.* **2006**, 361 (4), 687–697.

(42) Li, Z. G.; Wu, W. P.; Manolios, N. Structural mutations in the constant region of the T-cell antigen receptor (TCR)beta chain and their effect on TCR alpha and beta chain interaction. *Immunology* **1996**, 88 (4), 524–530.

(43) Garcia, K. C.; Teyton, L.; Wilson, I. A. Structural basis of T cell recognition. *Annu. Rev. Immunol.* **1999**, 17, 369–397.

(44) Beddoe, T.; Chen, Z.; Clements, C. S.; Ely, L. K.; Bushell, S. R.; Vivian, J. P.; Kjer-Nielsen, L.; Pang, S. S.; Dunstone, M. A.; Liu, Y. C.; Macdonald, W. A.; Perugini, M. A.; Wilce, M. C.; Burrows, S. R.; Purcell, A. W.; Tiganis, T.; Bottomley, S. P.; McCluskey, J.; Rossjohn, J. Antigen ligation triggers a conformational change within the constant domain of the alphabeta T cell receptor. *Immunity* **2009**, 30 (6), 777–788.

(45) van Boxel, G. I.; Holmes, S.; Fugger, L.; Jones, E. Y. An alternative conformation of the T-cell receptor alpha constant region. *J. Mol. Biol.* **2010**, 400 (4), 828–837.

(46) Harris, L. J.; Larson, S. B.; Hasel, K. W.; McPherson, A. Refined structure of an intact IgG2a monoclonal antibody. *Biochemistry* **1997**, 36 (7), 1581–1597.

(47) Wan, S.; Flower, D. R.; Coveney, P. V. Toward an atomistic understanding of the immune synapse: Large-scale molecular dynamics simulation of a membrane-embedded TCR-pMHC-CD4 complex. *Mol. Immunol.* **2008**, 45 (5), 1221–1230.

(48) Birnbaum, M. E.; Berry, R.; Hsiao, Y. S.; Chen, Z.; Shingu-Vazquez, M. A.; Yu, X.; Waghay, D.; Fischer, S.; McCluskey, J.; Rossjohn, J.; Walz, T.; Garcia, K. C. Molecular architecture of the alphabeta T cell receptor-CD3 complex. *Proc. Natl. Acad. Sci. U. S. A.* **2014**, 111 (49), 17576–17581.